

# Coronal Mass Ejections and Their Geospace Consequences

N. Gopalswamy

Center for Solar Physics and Space Weather  
The Catholic University of America  
Washington DC, USA  
and  
NASA/GSFC, Greenbelt, Maryland, USA

**Abstract.** I summarize the observed properties of CMEs and discuss two of their major consequences relevant to the geospace: geomagnetic storms and large solar energetic particle (SEP) events. The magnetic field structure of a CME essentially decides whether it can result in a geomagnetic storm. On the other hand, its shock-driving capability decides the production of SEPs. I also briefly discuss how advance warning of the arrival of CME related disturbances can be obtained. Finally, I touch upon the interacting CMEs, a new development in the study of the origin and propagation of CMEs.

## 1. Introduction

The connection between solar activity and geomagnetic disturbances was first recognized in the 19th century (Sabine, 1852; Carrington, 1860) and became well established in the early 20th century (Newton, 1943). Details of the connection emerged only after the discovery of coronal mass ejections (CMEs, Tousey, 1973) in the early 1970s (Gosling, 1993). Coronal holes are responsible for the recurrent geomagnetic storms with a period of 27 days (Chapman and Bartels, 1940). Coronal holes and CMEs are essentially the two solar phenomena responsible for most of the disturbed conditions in the geospace. Coronal holes contain open magnetic field lines that carry high-speed solar wind streams. CMEs originate from closed field regions on the Sun. The recurrent storms due to coronal holes are generally weaker than the non-recurrent storms caused by the CMEs. In this paper, we discuss only the geospace consequences of CMEs.

## 2. Basic Properties of CMEs

CMEs are large-scale magneto-plasma structures that erupt from the Sun and propagate through the interplanetary medium with speeds ranging from only a few  $\text{km s}^{-1}$  to nearly  $3000 \text{ km s}^{-1}$ . CMEs carry typically  $10^{15} \text{ g}$

of coronal material; a  $1500 \text{ km s}^{-1}$  CME, therefore, carries a kinetic energy of  $\sim 10^{31}$  erg. CMEs originate from active regions, filament regions or from complexes containing filaments and active regions. When a CME occurs, the closed magnetic structures are blown off, which expand into the inner heliosphere. Following a CME, the corona near the Sun restructures itself, producing post-eruption arcades or flare loops. A typical CME contains a frontal structure made of coronal material followed by material in the filament channel and the filament itself. As the eruption proceeds, the filament material may become partly or fully ionized. The heated filament becomes the core structure of many CMEs and lags behind the frontal structure (Gopalswamy et al., 1998). CMEs which appear to surround the occulting disks of white light coronagraphs are known as halo CMEs (Howard et al., 1982), which may be back-sided or front-sided. Those originating on the visible disk are also known as Earth-directed CMEs and are important from a space weather point of view. The mean angular width of CMEs is  $\sim 58^\circ$  (Gopalswamy et al., 2001a). CMEs are associated with a number of phenomena such as radio bursts, flares, prominence eruptions and solar energetic particles.

### 3. How are CMEs Observed?

CMEs are primarily observed by white light coronagraphs, which detect the Thomson-scattered photospheric light. By their very nature, the coronagraphs have an occulting disk to block the direct sun light, so they cannot observe the source regions of CMEs. We need non-coronagraphic observations to locate the region of eruption. H-alpha observations have been useful in identifying the solar sources. Two-ribbon flares, eruptive prominences and disappearing solar filaments are indicative of CME eruption. Inner coronal imaging in EUV and X-rays also provide information on solar sources of CMEs. Coronal dimming, arcade formation and EUV wave transients are excellent indicators of CMEs (Gopalswamy, 1999; Gopalswamy and Thompson, 2000). The WAVES experiment (Bougeret et al., 1995) on Wind spacecraft can detect type II radio bursts from large-scale CMEs when the CME is still close to the Sun (Gopalswamy et al., 2001a).

CMEs are also observed in situ as they blow past spacecraft in the solar wind. The interplanetary (IP) counterparts of CMEs are known as ICMEs, ejecta, or driver gas. A subset of the ICMEs is magnetic clouds (Burlaga et al., 1981), which are ejecta with higher than average magnetic field, smooth rotation of the field direction, and lower than average temperature. The magnetic clouds possess a flux rope structure as confirmed from multi-spacecraft observations in the IP medium (Burlaga et al., 1981). CMEs

moving faster than the local Alfvén speed can drive fast mode MHD shocks, which accelerate the electrons, protons, and ions of the solar wind to very high energies. The accelerated protons and heavier ions are known as solar energetic particles (SEPs). The energetic electrons are inferred from the type II radio bursts.

#### 4. Geospace Consequences of CMEs

The two primary geospace consequences of CMEs are the SEPs (depending on the energy of CMEs) and geomagnetic storms (depending on the structure of CMEs). The earliest effect of CMEs felt in the geospace is the arrival of SEPs in  $\sim 20$  minutes. This is followed by the arrival of the MHD shock and the CME which drives it. Sometimes, the shock continues to accelerate particles over the entire Sun-Earth connected space. CMEs may also arrive at 1 AU without shocks. In this section, we shall discuss the geomagnetic storms and the SEP in some detail.

##### 4.1 Geomagnetic Storms

Geomagnetic storms occur when the interplanetary magnetic field (e.g., those associated with ICMEs) impinges upon the Earth’s magnetosphere and reconnect (Dungey, 1961). Since the geomagnetic field is directed northward, the IP magnetic field needs to have a southward component for reconnection. When the reconnection occurs on the dayside, southward directed fields are convected to the nightside, where they reconnect once more in the Magnetospheric tail region, driving the tail plasma deep towards the Earth. This plasma injection is accompanied by the creation of plasma waves and energization of particles. Some of these energetic particles also cause the aurora. The drift of the energized electrons and ions in opposite directions results in the ring current around the Earth. The magnetic field associated with the ring current essentially reduces the geomagnetic field over a period of few days. The geomagnetic storms are thus characterized by the “Disturbance storm time” (Dst) index, which is an average of the horizontal component of Earth’s magnetic field measured at near-equatorial stations. When  $Dst < -50$  nT, the storm is considered moderate while it is severe when  $Dst < -100$  nT. During geomagnetic storms, particles in the magnetosphere can be energized to significant levels that they become hazardous to space-based technological systems and astronauts. Currents can also be induced in the ground, which may lead to the disruption of railroads and pipelines. Electric power transformers can be subject to huge surges resulting in their disruption.

Magnetic clouds contain southward field component either in its front

Table 1: CME travel time (days) for various initial speeds ( $\text{km s}^{-1}$ )

CME speed	travel time	CME speed	travel time
200	4.3	1500	1.5
400	4.3	2000	1.1
600	4.1	2500	0.8
1000	2.6	3000	0.7

or in the back. This ensures that the magnetic cloud will cause a geomagnetic storm. However, only about a third of all CMEs arriving at 1 AU are magnetic clouds. Whether or not a non-cloud ICME will result in a geomagnetic storm depends on the existence of a southward magnetic field component. When a CME is accompanied by a shock, the compressed region between the shock and the driving CME is known as the shock sheath. The sheath can also produce geomagnetic storms whenever it contains a southward magnetic field component.

Kinematic considerations show that Earth-directed CMEs arrive at 1 AU within 5 days of their departure near the Sun (Gopalswamy et al., 2000a). Based on an estimate of the IP acceleration that the CMEs undergo, an empirical model has been developed to predict the 1-AU arrival times of CMEs, given their initial speeds from remote sensing observations (Gopalswamy et al., 2001b). Although this model cannot tell us about the magnetic field orientation that the CMEs would eventually impose on the magnetosphere, it can provide a simple means of advance warning of the impending arrival of CMEs within a certain time window (less than a day). The empirical model predicts that Earth-directed CMEs starting out with a speed less than  $400 \text{ km s}^{-1}$  would arrive at 1 AU in about 4.3 days; CMEs leaving with higher speeds would arrive earlier, as indicated in Table 1 (extracted from Gopalswamy et al., 2001b).

#### 4.2 Large Solar Energetic Particle Events

It is known for quite some time that the large solar energetic particle (LSEP) events are closely related to CMEs (see, e.g., Reames, 1999; Tylka, 2001). This is because fast CMEs drive MHD shocks, which in turn accelerate the particles. LSEP events produce a proton flux of  $\sim 10$  pfu (particle flux units = particles per  $\text{cm}^2 \cdot \text{s} \cdot \text{sr}$ ) at the spacecraft. SEPs pose a severe radiation hazard in the geospace starting outward of low-Earth orbit. They can penetrate space suits of astronauts, destroy living cells and potentially cause cancer. SEPs also pose a major problem to spacecraft microelectronics and solar panels. When the shocks responsible LSEP events arrive

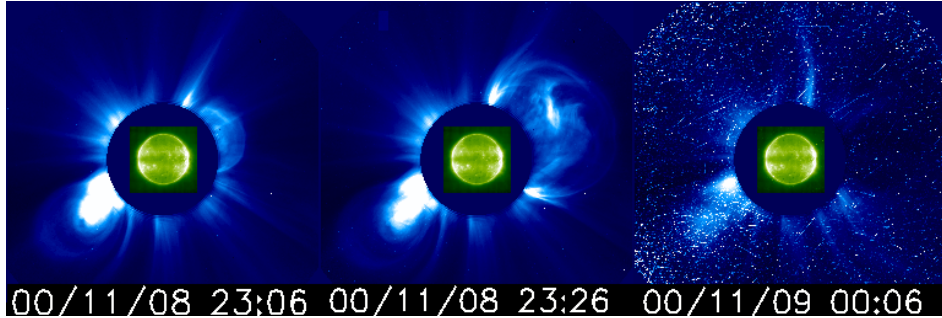


Figure 1: SOHO images of the CME (northwest quadrant) at three instances: when it first appears above the occulting disk (11/08/00 at 23:06 UT), just before leaving the coronagraph field of view (11/08/00 23:26 UT), and when the SEPs have already arrived at the SOHO detectors (11/09/00 at 00:06 UT), causing the ‘snow storm.’ EIT images are superposed to show the solar disk.

at 1 AU, they are accompanied by a population of lower energy particles accelerated locally. These are known as energetic storm particles (ESPs) and are also very geoeffective. We illustrate the effect of SEPs on space instrumentation using the 2000 November 08 CME detected by the Solar and Heliospheric Observatory (SOHO) mission’s Large Angle and Spectrometric Coronagraph (LASCO). The CME erupted from close to the west limb (N10 W77) moved out with a speed of  $1345 \text{ km s}^{-1}$ . The first two frames of Fig. 1 show the CME expanding above the west limb. In the third frame, the CME has left the field of view of the coronagraph. Note that this image is considerably degraded due to the arrival of SEPs at the SOHO detectors. The “snow storm” is a direct consequence of the SEPs and the image quality remained poor over the next day or so. The prompt arrival of SEPs was also recorded by the GOES satellite and the flux of  $> 10 \text{ MeV}$  protons increased by more than five orders of magnitude.

The Wind/WAVES experiment can detect the shocks responsible for the SEPs by observing the type II radio emission in the 1-14 MHz frequency range (Gopalswamy et al., 2000b). This frequency range corresponds to the decameter-hectometric (DH) wavelengths. It is a happy coincidence that the spectral range of the WAVES experiment corresponds to the field of view of the SOHO/LASCO coronagraph so that we can identify CME-driven shocks when they depart from the Sun. In a recent statistical study, Gopalswamy et al., (2001a) found that the DH type II bursts are due to faster and wider CMEs. Further investigation suggests that the WAVES

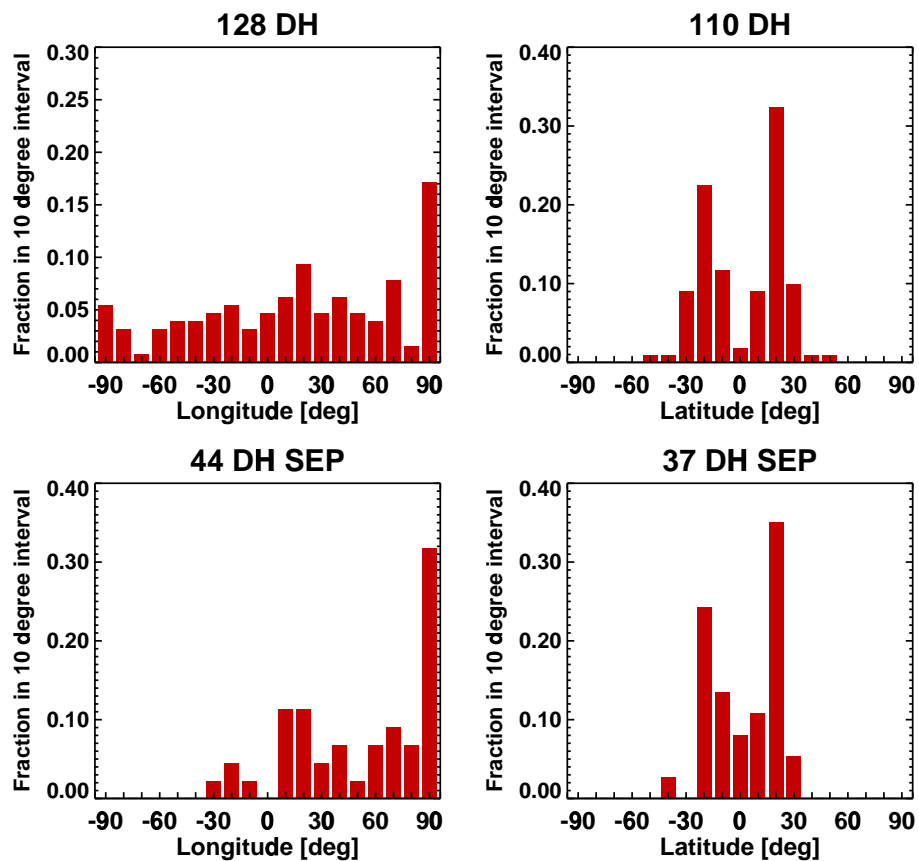


Figure 2: Histograms of the source longitudes and latitudes of 128 DH type II bursts and 44 large SEP events. The DH type II bursts were detected by the Wind/WAVES experiment. The SEP events were detected by the GOES satellite.

type II bursts are also indicators of LSEP events. To see this, we have compared the source regions of DH type II bursts and LSEP events. In Fig. 2, we have shown the source longitudes and latitudes for the 128 type II radio bursts in the DH domain along with those for the 44 LSEP events observed during the current solar cycle (until October 2001). We note that the latitudes of the sources are similar for the radio bursts and SEPs. The longitudinal distribution is also similar in both cases except that the LSEP events originate from longitudes west of E30. Thus DH type II bursts originating from the western hemisphere are good indicators of SEP accelerators.

### 5. New Developments and Future Prospects

The simple connection between solar eruptions and their geospace consequences gets complicated when CMEs interact. CMEs can collide with one another resulting in the change of trajectories or merger (Gopalswamy et al., 2001c). This will obviously result in counting different number of CMEs by remote sensing and in situ observations. The geomagnetic storms can become quite extended and complex when CMEs are ejected in quick succession. CME interaction has also important implications to particle acceleration. A continuum-like radio emission at  $\sim 3$  MHz was observed only during the interval of CME interaction on September 3, 1999 (Gopalswamy et al., 2001d). This requires acceleration of electrons during the interaction. In some cases, the slopes of radio bursts in the radio dynamic spectra show abrupt changes as a result of CME interaction. These observations suggest that CME interactions can result in shock-strengthening, creation of new shocks or reconnection far away from the Sun. Theories of SEP acceleration in shocks assume that the source material is from the normal solar wind. This is based on the fact that some LSEPs have charge states consistent with acceleration from the 1-2 million K coronal material. Recent observations have shown that most of the primary CMEs that accelerate LSEPs are preceded by one or more slower CMEs. This raises the interesting possibility that LSEPs are accelerated not from the quiet solar wind, but from the solar wind “contaminated” by the preceding CME material. Depending on the speed of the preceding CME, one can imagine multithermal, inhomogeneous source material entering into the shock to be accelerated. Thus the conventional shock-acceleration theories need to take into account of the CME interaction.

In conclusion, I would like to point out that CMEs constitute one of the primary factors influencing the non-recurrent dynamic conditions in the near-Earth space environment. Therefore, a clear understanding of the

interplanetary consequences of CMEs, is essential for any space exploration or other human activity involving space-based technological systems. For space weather purposes, Earth-directed CMEs are most relevant. Unfortunately, it is very difficult to measure the space speed of these CMEs from spacecraft located along the Sun-Earth line. Stereoscopic observations in the near future can overcome this problem. One still needs inner coronal imagers such as the Yohkoh soft X-ray telescope or SOHO's Extreme-ultraviolet imaging telescope to identify the solar sources of the Earth-directed CMEs. The traditional, ground-based H-alpha observations can also provide this information by proper networking of various observatories in the world.

**Acknowledgments:** The author thanks S. Yashiro for help with the figures. This research was supported by NASA, NSF and AFOSR.

### References

- Bougeret, J.-L. et al., 1995, *Space Sci. Rev.*, 71, 231.  
Burlaga, L., E. Sittler, F. Mariani, and R. Schwenn, 1981, *JGR*, 86, 6673.  
Carrington, R. C., 1860, *MNRAS*, 20, 13.  
Chapman, S. and J. Bartels, 1940, *Geomagnetism*, Oxford Univ. Press, Chap. 12.  
Dungey, J. W., 1961, *Phys. Rev. Lett.*, 6, 47.  
Gopalswamy, N., 1999, in NRO Report No. 479, p. 141.  
Gopalswamy, N. et al., 1998, *GRL*, 25, 2485.  
Gopalswamy, N. and B. J. Thompson, 2000, *JASTP*, 62, 1457.  
Gopalswamy, N., A. Lara, R. P. Lepping, et al., 2000a, *GRL*, 27, 145.  
Gopalswamy, N., et. al., 2000b, *GRL*, 27, 1427.  
Gopalswamy, N., S. Yashiro, M. L. Kaiser, et al. 2001a, *JGR*, 106, 29219.  
Gopalswamy, N., A. Lara, S. Yashiro, et al., 2001b, *JGR*, 106, 29207.  
Gopalswamy, N., S. Yashiro, M. L. Kaiser, et al., 2001c, *ApJ*, 548, L91.  
Gopalswamy, N., S. Yashiro, M. L. Kaiser, et al., 2001d, *GRL*, in press.  
Gosling, J. T., 1993, *JGR*, 98, 18,937.  
Howard, R. A., et al., 1982, *ApJ*, 263, L101.  
Newton, H. W., 1943, *MNRAS*, 103, 244.  
Reames, D., 1999, *Space Sci. Rev.*, 90, 413.  
Sabine, E., 1852, *Philos. Trans. R. Soc. London*, 142, 103.  
Tousey, R., 1973, *Adv. Space Res.*, 13, 713.  
Tylka, A., 2001, *JGR*, 106, 25,333.